

MODELLING STUDIES ON DICENTRICS INDUCTION AFTER SUB-MICROMETER FOCUSED ION BEAM GRID IRRADIATION

W. Friedland^{1,*}, P. Kundrát¹, E. Schmitt¹, J. Becker¹, K. Ilicic², C. Greubel³, J. Reindl³, C. Siebenwirth³, T.E. Schmid^{1,2} and G. Dollinger³

¹Department of Radiation Sciences, Helmholtz Zentrum München – German Research Center for Environmental Health, Neuherberg, Germany

²Department of Radiation Oncology, Technische Universität München, Munich, Germany

³Institute for Applied Physics and Metrology, Universität der Bundeswehr München, Neubiberg, Germany

Received month date year, amended month date year, accepted month date year

The biophysical simulation tool PARTRAC contains modules for DNA damage response representing non-homologous end joining of DNA double-strand breaks (DSB) and the formation of chromosomal aberrations. Individual DNA ends from the induced DSB are followed regarding both their enzymatic processing and spatial mobility, as is needed for chromosome aberrations to arise via ligating broken ends from different chromosomes. In particular, by tracking the genomic locations of the ligated fragments and the positions of centromeres, the induction of dicentrics can be modelled. In recent experiments, the impact of spatial clustering of DNA damage on dicentric yields has been assessed in *A_L* human-hamster hybrid cells: Defined numbers of 20 MeV protons (linear energy transfer, LET 2.6 keV/μm), 45 MeV Li ions (60 keV/μm) and 55 MeV C ions (310 keV/μm) focused to sub-μm spot sizes were applied with the ion microbeam SNAKE in diverse grid modes, keeping the absorbed dose constant. The impact of the μm-scaled spatial distribution of DSB (focusing effect) has thus been separated from nm-scaled DSB complexity (LET effect). The data provide a unique benchmark for the model calculations. Model and parameter refinements are described that enabled the simulations to largely reproduce both the LET-dependence and the focusing effect as well as the usual biphasic rejoining kinetics. The predictive power of the refined model has been benchmarked against dicentric yields for photon irradiation.

INTRODUCTION

The enhanced biological effectiveness of high-LET compared to low-LET radiation has been related to the clustering of DNA lesions⁽¹⁾. As experimental studies resolving DNA damage patterns on nanometer scales are not yet feasible, this finding is mainly based on track structure simulations that show increased lesion complexity in terms of DNA double-strand breaks (DSB), strand breaks, and damaged bases in close vicinity⁽²⁾. In the dose regime of medical applications there is another difference on a larger, (sub-)μm spatial scale: While DNA lesions from low-LET radiation are distributed randomly, high-LET radiation produces lesions highly non-homogeneously, along a few straight lines. Recently, the impact of this (sub-)μm-scaled difference on diverse biological endpoints has been addressed by innovative experiments with focused beams of protons mimicking single traversals of high-LET ions⁽³⁾: Compared with broad-beam proton irradiation, focusing 117 protons of 20 MeV energy (LET: 2.6 keV/μm) to sub-μm sized bunches increased the formation of micronuclei and dicentrics by factors of 1.2 and 1.6, respectively; however, these ratios were far below those (2 and 3.9) for single 55 MeV C ions (LET: 310 keV/μm) on the same quadratic grid of 5.4 μm × 5.4 μm. The enhancing effect on dicentrics was more

pronounced for higher numbers of protons on larger grids, and focusing Li ions in spots of 5, 10 and 20 ions with enlarged grids to keep the applied dose constant showed similar enhancements⁽⁴⁾.

The experiments with focused ion bunches provide unprecedented data for testing the underlying assumptions and improving the predictive power of mechanistic simulations. PARTRAC is a state-of-the-art tool for Monte Carlo simulations of radiation track structures, damage induction in cellular DNA, DSB repair via non-homologous end joining⁽⁵⁾ and induction of chromosomal aberrations (CA), in particular dicentrics⁽⁶⁾. Nanoscale DNA damage and its microscale distribution are explicitly considered. However, simulations with model assumptions and parameters used so far⁽⁶⁾ failed to properly match the focusing effect for protons and Li ions as well as the dependence on ion type (or LET) in single-ion irradiation modes^(4,7).

In this work, parameter studies with the PARTRAC CA model on existing^(3,4) and new data for C ions are reported. The simulations were aimed at reproducing the dependence of dicentric yields on ion type and focusing, maintaining consistence with biphasic repair kinetics as observed in experiments with unfocused ion beams^(8,9). To test its predictive power, the resulting model has been benchmarked against dose-dependent dicentrics after photon irradiation for *A_L* cells and human lymphocytes.

*Corresponding author: friedland@helmholtz-muenchen.de

METHODS

Experimental data

A_L hybrid cells, which contain the standard set of Chinese hamster ovary chromosomes plus a single copy of human chromosome 11 yielding a modal number of 21 chromosomes⁽¹⁰⁾, were irradiated at SNAKE by single ions or ion bunches in various regular grids with almost the same dose of ~ 1.7 Gy⁽⁴⁾. The bunch profile was approximately Gaussian with an elliptical shape with full width at half maximum of about $0.5 \times 1.0 \mu\text{m}^2$. Particle types, initial energies, grid sizes and numbers of ions per spot are listed in Table 1 together with measured yields of dicentrics per cell. New results for 1, 2 and 4 C ions on correspondingly increased grid sizes are presented together with earlier measurements^(3,4).

Table 1: Setup of experiments, measured dicentric yields and results of initial damage calculations with PARTRAC.

Ion type & energy (MeV)	Grid size (μm)	Ions per spot	Measured dicentrics per cell ($\pm\text{SE}$)	Calc. dose (Gy)	Calc. DSB per cell	Calc. dirty ends (%)
H 20 ⁺	0.5	1	0.047 \pm 0.009	1.72	54	38.5
H 20 ⁺	5.4	117	0.083 \pm 0.011	1.73	55	38.7
H 20 ⁺	7.6	232	0.114 \pm 0.016	1.74	55	39.0
H 20 ⁺	10.6	451	0.137 \pm 0.018	1.76	56	38.5
Li 45 ⁺	2.3	1	0.097 \pm 0.011	1.87	101	60.5
Li 45 ⁺	5.4	5	0.120 \pm 0.013	1.70	92	60.3
Li 45 ⁺	7.6	10	0.145 \pm 0.014	1.72	93	60.3
Li 45 ⁺	10.6	20	0.200 \pm 0.016	1.79	99	59.9
C 55 ⁺	5.4	1	0.197 \pm 0.012	1.81	130	84.2
C 55 ⁺	5.4	1	0.306 \pm 0.020	1.81	130	84.2
C 55 ⁺	7.6	2	0.191 \pm 0.020	1.83	134	84.2
C 55 ⁺	10.6	4	0.073 \pm 0.015	1.88	135	84.2

[†]earlier experiments⁽⁴⁾; ^{*}earlier experiments⁽³⁾

Simulation calculations with PARTRAC

The biophysical Monte Carlo tool PARTRAC⁽⁵⁾ has been used to calculate initial DNA damage after gridwise ion irradiation of spherical model nuclei with $10 \mu\text{m}$ diameter; details on methods and parameters of the simulation of ion-induced DNA damage have been reported elsewhere⁽¹¹⁾. All material traversed before reaching the cell⁽⁴⁾ and its biological matter were approximated by liquid water. A_L cell chromosomes were approximated by two copies of chromosomes 1-11 in a model of a human lymphocyte, yielding 4.22 Gbp total genomic length. Initial DNA damage patterns have been simulated in 1000 cells for 11 grid irradiation schemes corresponding to the experiments.

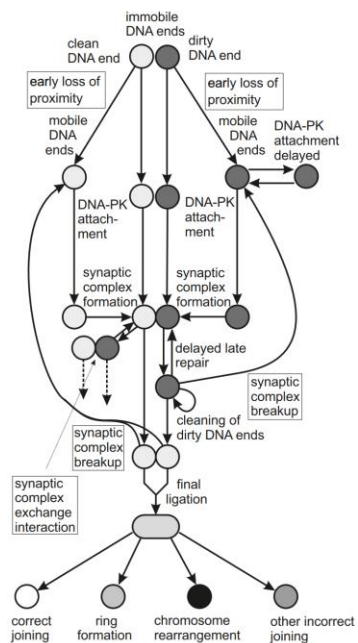


Figure 1. Scheme of DNA repair and CA model in PARTRAC. Different plausible mechanisms for misrejoining of broken DNA ends formed by DSB are indicated by boxes.

The DNA repair and CA model (Fig. 1) starts from the spatial distribution of individual ‘clean’ and ‘dirty’ DNA ends formed by DSB; dirty ends arise from nearby single-strand breaks and/or base lesions, while clean ends lack such additional damage. The model considers a mobilization step of DNA ends, e.g. by chromatin remodeling. Most immobile DNA ends create a synaptic complex with the previously linked end quickly after DNA-PK attachment; this leads to correct rejoining. Mobile ends and immobile ends with delayed DNA-PK attachment may diffuse away from their original partner before the synaptic complex is formed; this may lead to misrejoining events. Misrejoining also results from multiple DSB in close vicinity since very short DNA fragments (<25 bp) are assumed to be unrejoinable. Misrejoining of DNA ends from different chromosomes is mandatory for dicentrics formation.

Since earlier modelling attempts failed to reproduce both the impact of ion type and focusing on dicentrics yields after proton and Li ion irradiation⁽⁴⁾, in this work the hypotheses linked to misrejoining have been critically reviewed in numerous simulations aimed at matching the data in Table 1. First of all, model parameters have been varied that govern the classification of clean and dirty DNA ends into mobile

and immobile ones, which is crucial for the misrejoining mechanism described above, i.e. early loss of proximity between the partner DNA ends. Alternatively, plausible mechanisms have been considered that may act later during repair, namely break-up or mutual interaction of synaptic complexes (Fig. 1). Moreover, DNA end motion confined to the vicinity of nuclear attachment sites has been varied; it determines the balance between intra- and inter-chromosomal misrejoining during later repair phases. The influence of the assumed size of centromeres was tested too. Parameters on late repair kinetics have been adjusted to maintain the biphasic decrease of unrejoined DSB fractions, requiring that unrejoined DSB after 24 h depend on ion type stronger than on focusing. To help obtain such results, a grid of repair centers has been introduced that slightly attract free DNA ends. Time constants of the presynaptic phase, synopsis parameters, diffusion coefficients and further parameters were adopted as in earlier simulations^(4,6). For fragments up to a few kbp, joining of their ends has been suppressed; otherwise about 75% of total ring formation arise from such short fragments⁽⁶⁾.

Due to the stochastic nature, complexity and the related computational expensiveness of the simulations, standard optimization and sensitivity analyses could not have been performed. Instead, parameters in about 200 setups have been varied manually. Ranked by the sum of weighted squared deviations from the data, the best simulations matched in particular the focusing effect for protons.

To test its predictive capability, the model setup resulting from this optimization has been adopted for simulating dose-dependent dicentric yields for the same A_L cell line and human lymphocytes after X-ray and ^{60}Co γ -ray irradiations⁽¹²⁻¹⁴⁾.

RESULTS

The calculated yields of DSB and the fractions of dirty DNA ends listed in Table 1 are for a given dose fully determined by ion type and energy; they do not depend on focusing (grid size and number of ions per spot).

In many simulations on dicentrics, the focusing effect for protons and the LET effect between single Li ions and protons were overestimated as reported earlier⁽⁴⁾; this trend was rather robust against many variations. Both discrepancies were substantially reduced when the restrictions on DNA end mobility around the assumed nuclear attachment sites were relaxed to $\sim 0.8 \mu\text{m}$, independent of the genomic length to the free DNA end. The agreement with data has not been improved by considering break-up or interaction of synaptic complexes as major misrejoining mechanisms. Yet, a weak break-up contribution was needed to ensure that the fractions of unrejoined DSB 1 day post irradiation depend on LET stronger than on the focusing. Modifying the isotropic diffusive motion of DNA ends by a slight attractive force towards a grid of 'repair

centres' also acted in this direction. The best simulations with and without repair centres are compared to experimental data in Fig. 2.

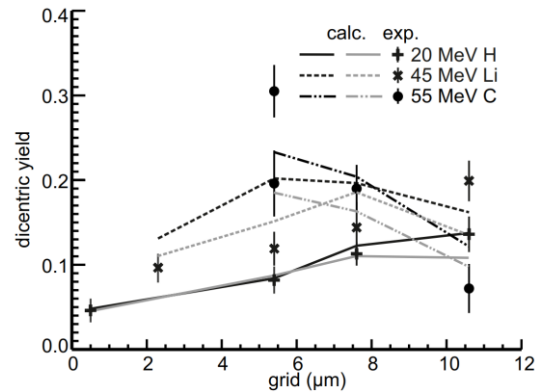


Figure 2. Yields of dicentrics in A_L cells after microbeam irradiation with focused ion beams. Symbols: experiments, black lines: calculation with repair centres, grey lines: calculation without repair centres.

Finally, dose-dependent yields of dicentrics after photon irradiation have been simulated and compared to measured data for A_L cells⁽¹²⁾ and lymphocytes^(13,14) (Fig. 3). These tests demonstrate that the reported model modifications have improved its predictive capability, since earlier calculations^(6,7) overestimated measured data by factors of 2 – 5.

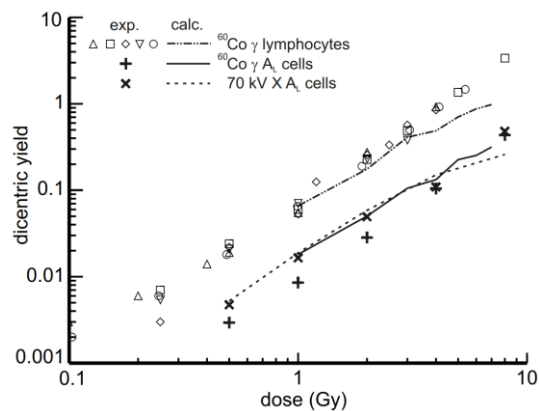


Figure 3. Measured dicentric yields in A_L cells⁽¹²⁾ after 70 kV X-ray and ^{60}Co γ -irradiation, and in human lymphocytes^(13,14) after ^{60}Co γ -irradiation, compared to PARTRAC calculations.

DISCUSSION AND CONCLUSION

The induction of dicentrics by focused ion beams has been utilized to improve the DNA repair and CA model of PARTRAC. Both the observed focusing and LET effects are reproduced far better than previously. Consideration of repair centres did not improve this

agreement but did help towards obtaining the (expected) LET-dependent kinetics. However, the increasing dicentric yields with increasing number of Li ions per spot could not be reproduced; virtually all performed simulations predict already for Li the inverted effect that, however, is observed for C ions only.

Simulations on dose-dependent induction of dicentrics in A_L cells after ⁶⁰Co γ-ray irradiation with the updated model show improved predictive capability, although around 1 Gy the measurements are exceeded by a factor of 2; at higher doses the deviation is reduced. Experiments with X-ray irradiation are well reproduced between 0.5 and 4 Gy by the simulations. However, the observed difference between 70 kV X-rays and ⁶⁰Co γ-rays is not reflected by the simulations. Simulations for human lymphocytes largely agree with experiments up to 3 Gy of ⁶⁰Co γ-rays. Dose-dependent yields for A_L cells and human lymphocytes run parallel in both the experimental data and simulations; however, the calculations underestimate the measured difference between the cell lines.

Approximating A_L chromosomes by two copies of human lymphocyte chromosomes 1-11 underestimates their genome size of about 90% of the genomic DNA in human cells⁽¹⁵⁾. Furthermore, three A_L chromosomes are rather large⁽¹⁰⁾, dissimilar to human cells. These differences might have influenced the simulated results, in particular regarding the cell-type dependences.

Taken together, the experiments with sub-μm focused beams continue to represent a challenge and a valuable benchmark to mechanistic modelling. The DNA repair and CA model in PARTRAC has been adjusted to better represent these experiments. The adjusted model shows improved predictive capabilities: It did not deviate from experiments by more than a factor of 2, including simulations for human lymphocytes after ⁶⁰Co γ-irradiation; tests for human cells after ion irradiation are ongoing. Additional work is needed to verify the model assumptions on the mobility of DNA ends and their processing. Comparison with data on repair foci or planned experiments on the temporal dimension of DNA lesion processing after sub-μm focused irradiation may help address this issue.

FUNDING

Supported by the project 'LET-Verbund' (funding no. 02NUK031C) of the German Federal Ministry of Education and Research.

REFERENCES

1. Goodhead, D.T. *Mechanisms for the effectiveness of high-LET radiations*. J. Radiat. Res. **40** (Suppl), 1-13 (1999).
2. Nikjoo, H., O'Neill, P., Terrissol, M. and Goodhead, D.T. *Quantitative modelling of DNA damage using Monte Carlo*

- track structure method*. Radiat. Environ. Biophys. **38**, 31-38 (1999).
3. Schmid, T.E. *et al. Low LET protons focused to submicrometer shows enhanced radiobiological effectiveness*. Phys. Med. Biol. **57**, 5889-5907 (2012).
4. Schmid, T.E. *et al. Sub-micrometer 20 MeV protons or 45 MeV lithium spot irradiation enhances yields of dicentric chromosomes due to clustering of DNA double-strand breaks*. Mutat. Res. **793**, 30-40 (2015).
5. Friedland, W., Dingfelder, M., Kunderát, P. and Jacob, P. *Track structures, DNA targets and radiation effects in the biophysical Monte Carlo simulation code PARTRAC*. Mutat. Res. **711**, 28-40 (2011).
6. Friedland, W. and Kunderát, P. *Track structure based modelling of chromosome aberrations after photon and alpha-particle irradiation*. Mutat. Res. **756**, 213-223 (2013).
7. Friedland, W., Kunderát, P. and Schmitt, E. *Modelling proton bunches focused to submicrometre scales: low-LET radiation damage in high-LET-like spatial structure*. Radiat. Prot. Dosim. **166**, 34-37 (2015).
8. Stenerlöw, B., Höglund, E., Carlsson, J. and Blomquist, E. *Rejoining of DNA fragments produced by radiations of different linear energy transfer*. Int. J. Radiat. Biol. **76**, 549-557 (2000).
9. Schmid, T.E. *et al. Differences in the kinetics of γ-H2AX fluorescence decay after exposure to low and high LET radiation*. Int. J. Radiat. Biol. **86**, 682-691 (2010).
10. Schmid, T.E. *et al. The effectiveness of 20 MeV protons at nanosecond pulse lengths in producing chromosome aberrations in human-hamster hybrid cells*. Radiat. Res. **175**, 719-727 (2011).
11. Friedland, W., Schmitt, E., Kunderát, P., Dingfelder, M., Baiocco, G. and Ottolenghi, A. *Comprehensive track-structure based evaluation of DNA damage by light ions from radiotherapy-relevant energies down to stopping*. Sci. Rep. **7**, 45161 (2017).
12. Schmid, T.E., Greubel, C., Dollinger, G. and Schmid, E. *The influence of reference radiation photon energy on high-LET RBE: comparison of human peripheral lymphocytes and human-hamster hybrid A_L cells*. Radiat. Environ. Biophys. **56**, 79-87 (2017).
13. Schmid, E., Ross, H. and Kramer, H.M. *The depth-dependence of the biological effectiveness of ⁶⁰Co gamma rays in a large absorber determined by dicentric chromosomes in human lymphocytes*. Radiat. Prot. Dosim. **130**, 442-446 (2008).
14. Bauchinger, M., Schmid, E. and Dresch, J. *Calculation of the dose-rate dependence of the dicentric yield after Co gamma-irradiation of human lymphocytes*. Int. J. Radiat. Biol. **35**, 229-233 (1979).
15. Gregory, T.R. *Animal genome size database*. <http://www.genomesize.com> (2017).